

Controlling the opto-mechanics of a cantilever in an interferometer via cavity loss

A. von Schmidsfeld^{a)} and M. Reichling^{b)}

Fachbereich Physik, Universität Osnabrück, Barbarastraße 7, 49076 Osnabrück, Germany

(Received 2 July 2015; accepted 14 September 2015; published online 24 September 2015)

In a non-contact atomic force microscope, based on interferometric cantilever displacement detection, the optical return loss of the system is tunable via the distance between the fiber end and the cantilever. We utilize this for tuning the interferometer from a predominant Michelson to a predominant Fabry-Pérot characteristics and introduce the Fabry-Pérot enhancement factor as a quantitative measure for multibeam interference in the cavity. This experimentally easily accessible and adjustable parameter provides a control of the opto-mechanical interaction between the cavity light field and the cantilever. The quantitative assessment of the light pressure acting on the cantilever oscillating in the cavity via the frequency shift allows an *in-situ* measurement of the cantilever stiffness with remarkable precision. © 2015 AIP Publishing LLC.

[<http://dx.doi.org/10.1063/1.4931702>]

A common method for measuring the displacement of a micro-cantilever or another micro-mechanical device is two beam interference in a Michelson interferometer using two mirrors for the superposition of two light beams.^{1,2} A related interferometric setup based on multi-beam interference in an optical cavity is the Fabry-Pérot interferometer typically used in form of an etalon in spectroscopy, lasers, and optical telecommunication³ for precise wavelength selection within a certain free spectral range.⁴ Conventionally, the Fabry-Pérot interferometer is characterized by the Finesse \mathcal{F} , defined as the ratio between the spectral selectivity and the free spectral range. Both types of interferometers are suitable for precisely detecting small movements of one of the involved mirrors.⁵ If the mirror has a small mass, the light can influence its movement via opto-mechanical coupling.⁶⁻⁸

The micro-cantilever used for force detection in an interferometry based non-contact atomic force microscope (NC-AFM)⁹ is a lightweight oscillating mirror in a cavity and, therefore, subject to forces originating from the radiation pressure acting on the cantilever.⁷ Under conditions of Fabry-Pérot interference, this yields an optical spring effect, i.e., an effective cantilever stiffness that is increased or lowered depending on the slope of the interference fringe.^{10,11} Here, we describe some aspects of the resulting opto-mechanical coupling and its influence on the dynamics of the cantilever oscillation and demonstrate that a variation of the optical loss of light in the cavity does not only allow a control of the interferometer but also an *in-situ* measurement of the cantilever stiffness with remarkable precision.

It is important to note that all our experiments are carried out at room temperature and with highly reflective cantilevers. This implies that the effects of opto-mechanical coupling reported here are due to photon pressure rather than bolometric effects,¹²⁻¹⁴ that dominate if the cantilever has a low reflectivity.¹⁵

Experiments are performed with a NC-AFM microscope body similar to the one introduced in Ref. 16 in an ultra-high vacuum environment with a base pressure of 3×10^{-11} mbar. The cleaved end of the optical fiber is positioned above the cantilever as shown in the photograph of Fig. 1(a) with an inertial stepper motor for coarse approach and a XYZ-tube-scanning-piezo for fine tuning exactly in the main maximum of the interference pattern with sub-nm precision. The alignment has to be precise to avoid excessive optical loss reducing or completely quenching Fabry-Pérot interference, whereas minor misalignment would increase the overall optical loss over the distance. The interferometer cavity is formed by the highly reflective back side of the cantilever and the partially reflecting cleaved end of the optical fiber. The aluminum coated silicon micro-cantilever used here (type NCLR, NanoWorld AG Neuchâtel, Switzerland) has a reflectivity of $R_c \approx 90\%$, dimensions of $l = 220 \mu\text{m}$, $w = 40 \mu\text{m}$, $t = 7 \mu\text{m}$, a nominal stiffness of $k_0^{\text{dim}} = (54 \pm 10)$ N/m (Refs. 17 and 18), and a measured eigenfrequency of $f_0 = 163\,941$ Hz at a temperature of 22.9°C . Determining the cantilever stiffness from the thermal peak¹⁹ yields a value of $k_0^{\text{th}} = (60 \pm 6)$ N/m. The stabilized laser light source (48TA-142037, Schäfter + Kirchoff GmbH, Hamburg, Germany) is operated at a wavelength of $\lambda = 782$ nm with the light power optimized for low noise operation. The power of the light coupled into the interferometer is optically adjusted by a variable absorber. The single mode optical fiber with a core diameter of $4.0 \mu\text{m}$ (type Hi780, Corning Inc., Corning, New York, USA) is optimized for transmission of light with the utilized wavelength. The fiber is cleaved with great care to achieve a measured interface reflectivity of $R_f = (3.9 \pm 0.3)\%$ that is within experimental error identical to the maximum possible value of 3.84% determined by the index of refraction of the fiber core material ($n = 1.48$ at 800 nm according to the data sheet). From the reflectivities, the maximum optical finesse of the cavity can be determined as $\mathcal{F} \approx \pi^4 \sqrt{R_c R_f} / (1 - \sqrt{R_c R_f}) = 1.7$. Our cavity design with a strong asymmetry in reflectivities enables us to operate the system equally well in the Fabry-Pérot and Michelson modes opposite to

^{a)}avonschm@uos.de

^{b)}reichling@uos.de

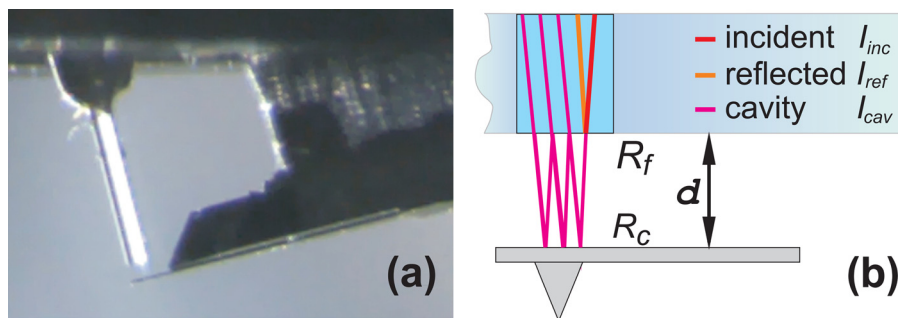


FIG. 1. (a) Photography of the interferometric detection setup in a non-contact atomic force microscope showing the optical fiber, the cantilever, and its support. The fiber end to cantilever distance d is set to $220\ \mu\text{m}$ to emphasize the cavity formed between the cantilever and the fiber end. (b) Sketch of the optical fiber supplying the incident beam with intensity I_{inc} and the internally reflected beam with intensity I_{ref} as well as a beam with intensity I_{cav} created by the optical field in the optical cavity.

systems optimized for Fabry-Pérot operation²⁰ or Michelson operation.²¹ By reducing the intensity in the reference beam of the Michelson interferometer while maintaining a high average reflectivity, we obtain a reasonable cavity finesse for the Fabry-Pérot mode. As a large fraction of the incident light is coupled into the cavity, we observe significant optomechanical effects in the Fabry-Pérot mode despite the relative low finesse.

The incident light intensity is measured at one output of a 3 dB coupler inserted between the laser and the fiber feeding the interferometer. The optical loss occurring in the feed line of the fiber to the microscope body has been quantified to be $f_{loss}^{fiber} = 0.44$ for each traversal, that has to be taken into account for the determination of incident and returning power. The high loss is mainly occurring in the tightly wound reserve coil inside the vacuum, containing about 3 m of fiber for new fiber-end cleaves and repairs. We make sure that the path length to the interferometer is larger than the coherence length of the laser to avoid interference in the connectors.

The optical fiber delivers light with intensity I_{inc} , while 3.9% of the incident light is reflected at the cleaved end yielding I_{ref} . The other part is coupled into the cavity and undergoes multiple reflections. The fraction of light that is collected by the fiber core from the cavity I_{cav} interferes with I_{ref} (Fig. 1(b)) to form the signal intensity I_{sig} . As the diameter of the fiber core is about five times the wavelength of the light, the light intensity distribution is dominated by pinhole diffraction leading to a diffraction limited aperture opening angle of 9° . The reflected light has the same divergence so that the fraction of the collected light is a measure for the cavity loss. The loss can be adjusted by the distance d between the fiber end and the cantilever as shown schematically in the inset of Fig. 2(b). Intensities are determined by measuring light power P_{inc} and P_{sig} by an optical power meter (type TQ8210, Advantest, Tokyo, Japan) and taking the reduction of the values by f_{loss}^{fiber} into account.

The plot of P_{sig} against the distance between fiber end and cantilever d shown in Fig. 2(a) yields a characteristic decrease of the mean returned power P_{mean} due to the optical loss increasing with the distance superimposed by oscillations appearing in the two regimes of predominant Fabry-Pérot and Michelson interference. The oscillations describe the modulation between intensity maxima P_{max} (red) and minima P_{min}

(green) yielding the mean intensity $P_{mean} = \frac{1}{2}(P_{max} + P_{min})$ (light gray) that asymptotically approaches the power P_{ref} determined by the fiber end reflectivity R_f . Note, however, that the oscillation period does not reflect the ratio between wavelength and cavity length but is caused by aliasing effects of the coarse fiber positioning stepper having a step size of $400\ \text{nm}$ with the fringes of the interferometer appearing every $97.75\ \text{nm}$. The curves for P_{min} , P_{max} , and P_{mean} shown in Fig. 2(a) are determined as envelopes of P_{sig} . By fine tuning d with sub-nm precision with the tube piezo, we avoid missing any

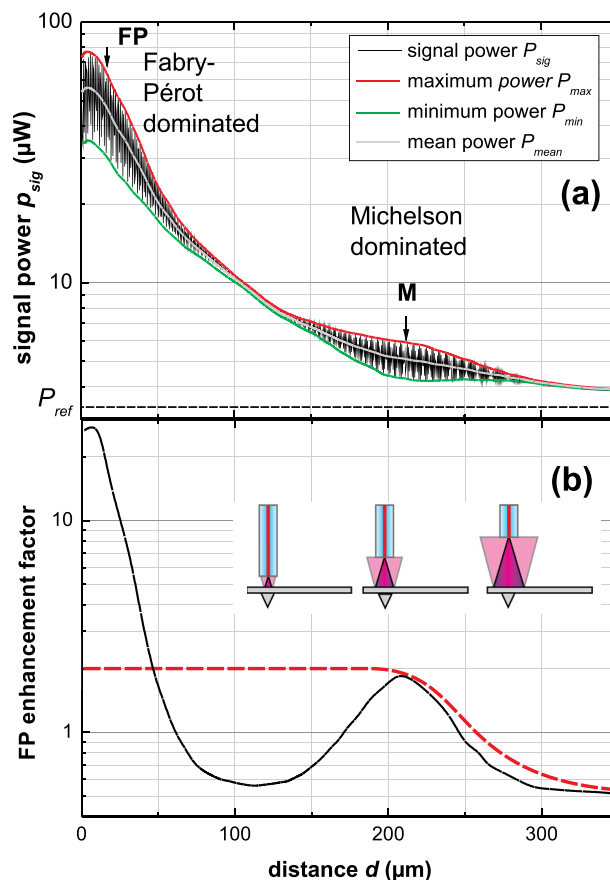


FIG. 2. (a) Signal power (black) with maximum (red), minimum (green), mean (light gray), and reference beam (dashed line) power as a function of the distance d between fiber end and cantilever. (b) Fabry-Pérot enhancement factor \mathcal{F} (black) with model curve for Michelson interference (dashed red line). Inset sketch of optical losses with arbitrary intensity reflected back into the fiber core as well as $1/4$ and $1/9$ thereof.

maximum or minimum and check the distance calibration intrinsically provided by the wavelength.

The finesse \mathcal{F} is also a measure for the cavity light field amplification. In an NC-AFM setup, this parameter is difficult to determine experimentally as well as the absolute value of the optical loss. Therefore, we introduce a closely related characteristic property of the interferometer derived from the measured optical response that is further on referred to as *Fabry-Pérot enhancement factor* $\tilde{\mathcal{F}}$ based on the light power acting on the cantilever in relation to the power reflected at the fiber end P_{ref}

$$\tilde{\mathcal{F}} = \frac{P_{max} - P_{min}}{P_{ref}} \times e^{\left(\frac{P_{max} - P_{min} - 2P_{ref}}{P_{ref}}\right)}. \quad (1)$$

Note that $\tilde{\mathcal{F}}$ is based on relative power values of light returned from the fiber end and the cavity and is, therefore, not affected by the optical loss in the feed line. This quantity is extracted from the measurement shown in Fig. 2(a) and plotted versus d in Fig. 2(b).

For all practical purposes, the enhancement factor $\tilde{\mathcal{F}}$ behaves similar to the finesse \mathcal{F} , however, it takes the reduction of the light intensity due to all cavity losses into account. In case of negligible optical loss (at very small distances d), $\tilde{\mathcal{F}}$ approximates \mathcal{F} , except for a factor depending on the fiber end reflectivity R_f

$$\tilde{\mathcal{F}} \rightarrow \frac{1 - R_f}{R_f} \frac{2}{\pi} \mathcal{F} + 1 \text{ for } d \rightarrow 0. \quad (2)$$

This can be interpreted as a calibration of the light energy stored in the cavity not against the incoming beam intensity, but against the reflected beam intensity.

For small d , $\tilde{\mathcal{F}}$ is larger than 25 clearly indicating predominant Fabry-Pérot characteristics, as the maximum for two beam interference of a Michelson interferometer is $\tilde{\mathcal{F}} = 2$ as indicated by the red dotted line in Fig. 2(b). This can be understood by considering an ideal Michelson interferometer having two equally strong beams interfering with a modulation depth of $M = 100\%$, resulting in $P_{max} = 2P_{ref}$ and $P_{min} = 0$. This is achieved when the power coupled back into the fiber from the cavity P_{cav} is equal to the power of the reference beam P_{ref} reflected inside the fiber. In the distance region between the Fabry-Pérot and Michelson regimes, ($d \approx 110 \mu\text{m}$), the interferometric signal is effectively quenched as the signals originating from the FP mode and the M mode have similar amplitude but 180° phase shift.

A study of the opto-mechanical coupling in dependence of the interference conditions is best accomplished by exciting the cantilever to oscillation at its resonance frequency f_{res} by a piezo element driven at constant excitation voltage V_{exc} . As the cantilever oscillates in the spatially sinusoidally modulated light field of the cavity, the opto-mechanical force due to the radiation pressure acting on the cantilever⁷ varies sinusoidally over the fringe and influences the cantilever dynamics resulting in a shift of f_{res} with respect to its eigenfrequency f_0 . The modification of the restoring force of the cantilever can be described analogue to the one of a pendulum, exhibiting an amplitude dependent frequency shift due

to the sinusoidal variation of the gravity-induced force component as a function of pendulum deflection.²²

The oscillation amplitude dependent frequency shift is observed also in our experiments, for instance, in Fig. 3 where the frequency shift $df = f_0 - f_{res}$ is plotted against the excitation voltage V_{exc} for measurements in the two interferometric regimes of interest. In each measurement, the interferometer is first adjusted to the point of maximum slope of a positive fringe and then to the maximum slope of a neighboring negative fringe. At position **M** ($d = 210 \mu\text{m}$) representing Michelson dominated interference, the frequency shift is small and equal for both fringes as expected since the spatial modulation of the light intensity in the cavity is weak. A maximum shift of $df_M^\pm = -0.11 \text{ Hz}$ is observed for an excitation voltage $V_{exc}^{\lambda/8}$ corresponding to a cantilever oscillation amplitude of half of the fringe width. In the **FP** region ($d = 20 \mu\text{m}$) representing Fabry-Pérot dominated interference, the frequency shift increases to -1.31 Hz for the negative fringe and to -1.48 Hz for the positive fringe due to the cavity amplification of the light field interacting with the cantilever.

The fringe-dependent shift in the resonance frequency has been observed before and is explained by the different directions of the optical force gradient.⁸ The split of the frequency shift for positive and negative fringes is evidence for light pressure governing the opto-mechanical coupling between the cantilever and the cavity light. This is expected as the highly reflective cantilever absorbs only a small fraction of the incident light, yielding negligible bolometric effects. Our measurements allow a quantification of the light pressure acting on the cantilever, by adjusting V_{exc} so that the oscillation covers exactly one fringe, i.e., an oscillation amplitude of $A_{\lambda/8} = 97.75 \text{ nm}$. The maximum force acting on the cantilever is reached at a turning point of the oscillation, and we can relate the maximum opto-mechanical force F_O to the maximum restoring force of the bent cantilever F^\pm depending on its effective stiffness k^\pm for the respective fringe. The ratio between F_O and F^\pm can be derived from the frequency shift $\delta f_{\lambda/8}^\pm$ corresponding to $V_{exc}^{\lambda/8}$, following the

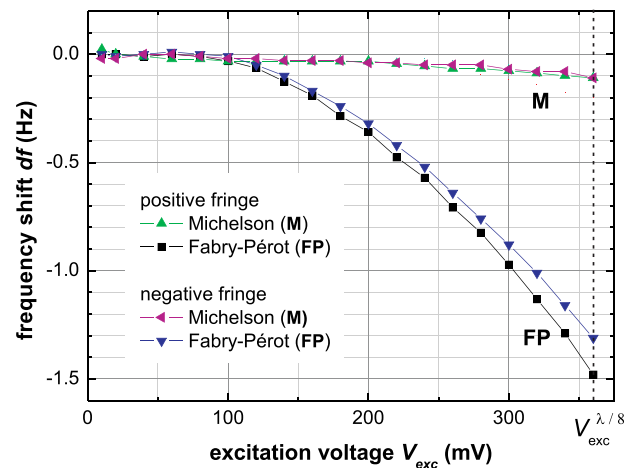


FIG. 3. Frequency shift df plotted as a function of the cantilever excitation voltage V_{exc} for both fringes of Michelson and Fabry-Pérot interferometer configurations. Strong opto-mechanical interaction is evident in the Fabry-Pérot regime (black squares and blue triangles) but much weaker in the Michelson regime (green and magenta triangles).

derivation outlined in the supplementary material.²³ Based on the formalism describing the maximum frequency shift of 18% observed for the pendulum with 90° deflection,²² we find

$$\frac{F_O}{F^\pm} = \frac{k_O}{k^\pm} \approx -2 \frac{\delta f_{\lambda/8}^\pm}{f_0} (1 + 0.18)^2, \quad (3)$$

where k_O is the stiffness contribution due to the opto-mechanical coupling. As the Fabry-Pérot enhancement factor of the cavity quantifying the light acting on the cantilever compared to the reference beam can straightforwardly be determined and P_{ref} is known, we can calculate the force exerted by the radiation pressure on the reflective cantilever

$$F_O = \frac{1}{1 - f_{loss}^{fiber}} \times \frac{2P_{ref}}{c} \times \tilde{\mathcal{F}}. \quad (4)$$

Here, we neglect the momentum transferred by photons absorbed in the cantilever, which is a valid approximation for a highly reflective cantilever. This allows a straightforward determination of the effective cantilever stiffness for positive and negative fringes, respectively,

$$\begin{aligned} k^\pm &= \frac{F^\pm}{F_O} \times F_O \times A_{\lambda/8}^{-1} \\ &= -\frac{1}{2} \frac{f_0}{\delta f_{\lambda/8}^\pm} (1 + 0.18)^{-2} \times \frac{1}{1 - f_{loss}^{fiber}} \frac{2P_{ref}}{c} \tilde{\mathcal{F}} \times \frac{8}{\lambda}. \end{aligned} \quad (5)$$

For the cantilever used here, the spring constant obtained by this method in the Michelson regime **M** is $k_M^\pm = 56.1 \pm 1.0$ N/m. In the Fabry-Pérot regime **FP**, the stiffness is fringe dependent; and we find $k_{FP}^+ = 58.7 \pm 0.6$ N/m for the positive fringe and $k_{FP}^- = 52.0 \pm 0.6$ N/m for the negative fringe yielding a change of ± 3.3 N/m in the effective spring constant by the optical spring effect from the mean value of $k_{mean} = 55.4 \pm 0.6$ N/m. As mechanical and optical force constants are superimposed linearly, a measurement for both fringes allows a straightforward calculation of the intrinsic cantilever stiffness as $k = \frac{1}{2}(k + k_O + k - k_O) = \frac{1}{2}(k^+ + k^-) = k_{mean}$. The symmetry of the results for positive and negative fringes is a clear-cut proof that bolometric effects are negligible in our case and the precision of the measurement is basically limited by the accuracy in determining the reference light power P_{ref} and the fiber loss f_{loss}^{fiber} .

We point out that the cantilever stiffness can be determined even if the Fabry-Pérot enhancement factor has been determined for an interferometer configuration that is different from the one of cantilever operation. To accomplish this, $\tilde{\mathcal{F}}$ is calculated by comparing the mean frequency shift $\overline{\delta f} = \frac{1}{2}(\delta f^+ + \delta f^-)$, to a reference frequency shift $\overline{\delta f}_{ref} = \frac{1}{2}(\delta f_{ref}^+ + \delta f_{ref}^-)$ measured in a configuration of known $\tilde{\mathcal{F}}_{ref}$ that can be an arbitrary operating point of the interferometer. From Eq. (5), we find

$$\tilde{\mathcal{F}} \approx \tilde{\mathcal{F}}_{ref} \frac{\overline{\delta f}}{\overline{\delta f}_{ref}}. \quad (6)$$

A good reference point is position **M** at $d = 210 \mu\text{m}$ where we find $\delta f_{ref} = -0.11$ Hz and $\tilde{\mathcal{F}}_{ref} = 1.9$, whereas at position **FP** the shift is -1.48 Hz. Using the **M** reference data, we

find $\tilde{\mathcal{F}}_{FP} = 26.9$ at $d = 20 \mu\text{m}$, and this is within the experimental error identical with the theoretical upper limit of $\tilde{\mathcal{F}}_{max} = 26.8$ determined by the Finesse \mathcal{F} calculated from the reflectivities for negligible cavity loss

$$\tilde{\mathcal{F}}_{max} \approx \frac{1 - R_f}{R_f} \frac{2}{\pi} \times \frac{\pi \sqrt[4]{R_c R_f}}{1 - \sqrt{R_c R_f}} + 1. \quad (7)$$

In conclusion, by using a cantilever with reflective coating, it is possible to generate multi-beam interference in a well aligned cavity formed by the fiber end and a cantilever. The strength of this multi-beam interference can be tuned over a wide range by the cavity loss varied via the fiber-cantilever distance where the interference character can be changed from a predominantly Fabry-Pérot to predominantly Michelson.

For the case of multi-beam interference, the interaction between the cavity-amplified optical field and the cantilever results in opto-mechanical coupling and a shift of the resonance frequency of the cantilever. The Fabry-Pérot enhancement factor, that is a quantitative measure for the cavity loss, can be determined via simple measurements of the oscillation amplitude dependent frequency shift and returned light power in the detection arm. This, further, allows a determination of the effective cantilever force constant for operation in positive and negative fringes as well as the intrinsic cantilever stiffness with remarkable precision. The fringe dependent increased or decreased stiffness is due to the optical spring effect of the radiation pressure for a cavity with a highly reflective cantilever. If the cantilever stiffness has been already determined precisely by another method, this measurement can also be reversed to determine the amount of sinusoidally modulated light present in the cavity interacting with the cantilever. Properly positioning the cantilever in the modulated light field and varying the amount of light stored in the cavity in more sophisticated experiments will allow the control of the cantilever motion in phase space what is, for instance, desirable for optimizing the cantilever response in NC-AFM measurements.

The authors are grateful to Alexander Schwarz for most fruitful discussions.

¹P. R. Saulson, *Phys. Rev. D* **42**, 2437 (1990).

²C. A. J. Putman, B. G. Degrooth, N. F. Vanhulst, and J. Greve, *Ultramicroscopy* **42-44**, 1509 (1992).

³R. Boucher, B. Villeneuve, M. Breton, and M. Ttu, *Photonics Technol. Lett.* **4**, 801 (1992).

⁴J. Stone and L. W. Stulz, *Electron. Lett.* **23**, 781 (1987).

⁵L.-H. Shyu, C.-P. Chang, and Y.-C. Wang, *Rev. Sci. Instrum.* **82**, 063103 (2011).

⁶I. Favero and K. Karrai, *Nat. Photonics* **3**, 201 (2009).

⁷T. J. Kippenberg and K. J. Vahala, *Science* **321**, 1172 (2008).

⁸L. Tröger and M. Reichling, *Appl. Phys. Lett.* **97**, 213105 (2010).

⁹B. Kracke and B. Damaschke, *Rev. Sci. Instrum.* **67**, 2957 (1996).

¹⁰V. B. Braginsky, S. E. Strigin, and S. P. Vyatchanin, *Phys. Lett. A* **287**, 331 (2001).

¹¹T. J. Kippenberg, H. Rokhsari, T. Carmon, A. Scherer, and K. J. Vahala, *Phys. Rev. Lett.* **95**, 033901 (2005).

¹²C. H. Metzger and K. Karrai, *Nature* **432**, 1002 (2004).

¹³M. Vogel, C. Mooser, K. Karrai, and R. J. Warburton, *Appl. Phys. Lett.* **83**(7), 1337 (2003).

- ¹⁴G. Flaschner, K. Ruschmeier, A. Schwarz, M. R. Bakhtiari, M. Thorwart, and R. Wiesendanger, *Appl. Phys. Lett.* **106**, 123102 (2015).
- ¹⁵H. Hölscher, P. Milde, U. Zerweck, L. M. Eng, and R. Hoffmann, *Appl. Phys. Lett.* **94**, 223514 (2009).
- ¹⁶W. Allers, A. Schwarz, U. D. Schwarz, and R. Wiesendanger, *Rev. Sci. Instrum.* **69**, 221 (1998).
- ¹⁷J. Lübke, L. Doering, and M. Reichling, *Meas. Sci. Technol.* **23**, 045401 (2012).
- ¹⁸J. Lübke, M. Temmen, H. Schnieder, and M. Reichling, *Meas. Sci. Technol.* **22**, 055501 (2011).
- ¹⁹J. Lübke, M. Temmen, P. Rahe, A. Kühnle, and M. Reichling, *Beilstein J. Nanotechnol.* **4**, 227 (2013).
- ²⁰B. W. Hoogenboom, P. L. T. M. Frederix, J. L. Yang, S. Martin, Y. Pellmont, M. Steinacher, S. Zach, E. Langenbach, H. J. Heimbeck, A. Engel, and H. J. Hug, *Appl. Phys. Lett.* **86**, 074101 (2005).
- ²¹D. Rugar, H. J. Mamin, and P. Guethner, *Appl. Phys. Lett.* **55**, 2588 (1989).
- ²²K. Ochs, *Eur. J. Phys.* **32**, 479 (2011).
- ²³See supplementary material at <http://dx.doi.org/10.1063/1.4931702> for derivation of formula (3).